Available online at www.sciencedirect.com

ScienceDirect

IFAC-PapersOnLine 49-17 (2016) 242–247

Aggressive Turn-Around Manoeuvres with an Agile Fixed-Wing UAV

Joshua M. Levin * **Meyer Nahon** ** **Aditya A. Paranjape** ***

* *Mechanical Engineering Department, McGill University, Montreal, Canada (e-mail: joshua.levin@mail.mcgill.ca).*
** *Mechanical Engineering Department, McGill University, Montreal, Canada (e-mail: meyer.nahon@mcgill.ca)*
*** *Department of Aerospace Engineering, IIT Bombay, Powai, Mumbai, India (e-mail: paranjape@aero.iitb.ac.in)*

Abstract:
This paper investigates an aerobatic manoeuvre performed by an agile fixed-wing unmanned aerial vehicle, with the intent of determining how best the manoeuvre can be automated. The manoeuvre is an aggressive turn-around: a 180 degree reversal of the aircraft's heading, in which the space required for completing the turn is minimized. A comprehensive dynamics model of an agile fixed-wing aircraft is used to design trajectories of the manoeuvre off-line using optimal control. A methodology for evaluating the suitability of controllers for executing the manoeuvre is also presented.

Keywords: Manoeuvrability, Agile Control, Aerospace Trajectories, Optimal Control, Optimal Trajectory, Optimality, Optimization Problems.

Fig. 1. Electrifly by Great Planes Yak54 3D RC plane

1. INTRODUCTION

The use of unmanned aerial vehicles (UAVs) has grown dramatically over the past decade. While they were originally driven by military applications, they are now proposed for uses as diverse as detection and mapping of forest fires; monitoring of long distance power lines or pipelines in remote areas; aerial search and rescue; wildlife monitoring; road traffic monitoring; and police surveillance. Mainstream UAVs typically fall into one of two categories: fixed-wing or rotorcraft. Rotorcraft are usually chosen for tasks that make use of their ability to handle precisely at low speeds and stop mid-flight, however, they lack the endurance of fixed-wing aircraft. Advancements in research have begun to bridge the gap between these two categories of UAVs by increasing the agility of fixed-wing aircraft, and in so doing, broadening their suitability for missions requiring endurance *and* manoeuvreability.

Agile fixed-wing UAVs, one pictured in Figure 1, are capable of very impressive performance, as becomes evident when observing the extreme manoeuvres that can be performed by radio control (RC) pilots. Not only are these extreme manoeuvres spectacular, they are functionally significant. For instance, avoiding obstacles in constrained environments - such as forests and urban areas - requires rapid transient motions. The manoeuvre of interest, an aggressive turn-around (ATA), finds its usefulness in retreating from dead ends, among other applications. These capabilities, however, are rarely exploited by users of small UAVs due to the high complexity of piloting inputs that this entails - whether by a human teleoperator, or, even more so, by an automatic control system.

The study of the automation of aerobatic manoeuvres with fixed-wing UAVs is in its infancy. Most research in this area has focused on hovering and perching manoeuvres; see Green and Oh (2005), and Cory and Tedrake (2008). Little work, however, has been done to automate other agile manoeuvres. In Matsumoto et al. (2010), the authors designed a turn-around manoeuvre in which the aircraft first pulls its flight path angle up to nearly 90 degrees, then performs a 180 degree roll, drops its nose and recovers to level flight. The optimization problem they solved, and hence the manoeuvre, was restricted to two dimensions.

We approach the problem of automating an aggressive turn-around by investigating the dynamics of the manoeuvre, revealed in trajectories generated using optimal control theory, similar to the work of Cory and Tedrake (2007). Through this approach we are able to understand the full capabilities of the aircraft, and how closely a feedback controller can get the aircraft to those ultimate performance bounds.

The paper is organized as follows. Section 2 introduces the optimal control problem, presents the aircraft dynamics model, and discusses results. Section 3 reformulates the optimal control problem by introducing feedback control

Peer review under responsibility of International Federation of Automatic Control.
10.1016/j.ifacol.2016.09.042

laws and examines the results in comparison to those of Section 2.

2. OPTIMAL CONTROL

Trajectories were generated off-line by defining the ATA manoeuvre as the solution to an optimal control problem, which outputs the time histories of the motion variables and control inputs (thrust, and deflections in aileron, elevator, and rudder surfaces) throughout the manoeuvre.

2.1 Aircraft Dynamics Model

The aircraft dynamics model used in this paper was largely derived from the work of Khan (2016), which thoroughly models agile fixed-wing UAV dynamics over their full flight envelope. This work addresses all of the most relevant factors that influence an aircraft's flight behavior, namely: thruster dynamics, slipstream effects, and aerodynamics. Any deviations from this model were embraced in favor of computational efficiency during optimal control. The specific aircraft configuration used for this research is an Electrifly by Great Planes Yak54 3D RC plane, seen in Figure 1. The mass, inertia, and geometric properties used in the model are attributed to this UAV.

The ordinary differential equations of motion for a rigid aircraft are as follows:

$$\begin{aligned} \dot{\mathbf{V}}_B &= \frac{1}{m}\mathbf{F}_B - \boldsymbol{\omega}_B^{\times}\mathbf{V}_B \\ \dot{\boldsymbol{\omega}}_B &= \mathbf{I}_B^{-1}[\mathbf{M}_B - \boldsymbol{\omega}_B^{\times}\mathbf{I}_B\boldsymbol{\omega}_B] \\ \dot{\mathbf{C}}_{BI} &= -\boldsymbol{\omega}_B^{\times}\mathbf{C}_{BI} \\ \dot{\mathbf{r}}_I &= \mathbf{C}_{BI}^{\mathsf{T}}\mathbf{V}_B \end{aligned} \tag{1}$$

where $\boldsymbol{V}_B = [u, v, w]^{\mathsf{T}}$ and $\boldsymbol{\omega}_B = [p, q, r]^{\mathsf{T}}$ are the translational and angular velocity of the aircraft resolved in the body frame, which is fixed to the aircraft and has origin at the aircraft's center of gravity. The inertia matrix, $\mathbf{I}_B$, is also resolved in the body frame, while the gravity and position vectors, $\mathbf{g}_I$ and $\boldsymbol{r}_I = [x, y, z]^{\mathsf{T}}$, are resolved in the inertial frame. Note that:

$$\boldsymbol{\omega}_B^{\times} = \begin{bmatrix} 0 & -r & q \\ r & 0 & -p \\ -q & p & 0 \end{bmatrix} \tag{2}$$

The term $\mathbf{C}_{BI}$ is the rotation matrix that parametrizes the attitude of the body frame relative to the inertial frame. It is composed of three rotations about the primary axes; roll, ϕ, about the x-axis, pitch, θ, about the y-axis, and yaw, ψ, about the z-axis:

$$\mathbf{C}_{BI} = \mathbf{C}_1(\phi)\mathbf{C}_2(\theta)\mathbf{C}_3(\psi) \tag{3}$$

The net forces and moments acting on the aircraft, $\mathbf{F}_B$ and $\mathbf{M}_B$, have three sources: gravity, propulsion, and aerodynamics.

Thruster Model The effects of propulsion generated by the aircraft's thruster are accounted for in this portion of the model. The thruster model accepts three inputs: thrust, translational velocity, and angular velocity. It outputs the forces and moments, both aerodynamic and gyroscopic, created by the thruster unit (in the body frame), $\mathbf{F}_{B,T}$ and $\mathbf{M}_{B,T}$. Forces and moments are predicted under all flow conditions: static, axial, oblique, and reverse flow. All components of an electric-powered UAV thruster are considered, namely: the battery, electronic speed controller, brushless DC motor, and propeller. The velocity induced by the rotating propeller is also calculated for use in the slipstream model. The full details of the thruster dynamics - which are employed here in their entirety - are found in Khan and Nahon (2013).

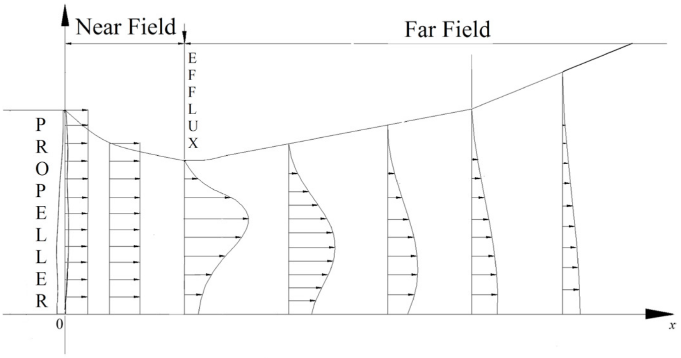

Fig. 2. Propeller slipstream: near field and far field regions

Propeller Slipstream Model The propeller slipstream effect is a key component in the modeling of agile UAVs since it provides additional airflow over the control surfaces, which can be crucial in aggressive manoeuvreing, especially at low speeds. The output of the slipstream model is the velocity of this additional airflow in the axial direction; the tangential and radial components are negligible. The axial airflow term is calculated differently for two regions: a near-field region and a far-field region, which are separated at the 'efflux plane', measured axially from the location of the propeller, as seen in Figure 2. The aircraft's fuselage and part of its main wing (that which is closest to the fuselage) reside in the near-field region. In this region the axial airflow's motion is dominated by the pressure force created by the propeller, which induces an acceleration. The airflow here is calculated using momentum theory, which is conventionally - and less accurately - used for representing the entire slipstream effect. The horizontal and vertical tail wings are located in the far-field region; this section of the model is both significant and novel. In this region, air viscosity and turbulence become more prominent and cause diffusion of the slipstream radially into the ambient flow. As a result of the momentum transfer between the fast-moving slipstream and the slow-moving ambient flow, the slipstream velocity decreases. In the far-field region, the slipstream velocity profile is calculated via a one-term Gaussian function to account for this diffusion phenomenon. The slipstream effect also includes a swirl component. This effect is modeled as a reduction of 60% on the thruster's reaction torque, $\mathbf{M}_{B,T_x}$. Refer to Khan and Nahon (2015) for a complete explanation of the slipstream model.

Aerodynamics Aerodynamic forces and moments are determined using a component breakdown approach that, in this paper, uses the following segments: starboard main